Reduced and Redundant: Information Processing of Prediction Errors during Sleep

Christine Blume[1,2,3][0000-0003-2328-9612], Marina Dauphin[4], Maria Niedernhuber[4][0000-0002-4459-6796], Manuel Spitschan[5,6][0000-0002-8572-9268], Martin P. Meyer[0000-0002-8041 5884], Christian Cajochen[1,2]§[0000-0003-2699-7171], Tristan Bekinschtein[4]§[0000-0001-5501-8628], Andrés Canales-Johnson[4,8]§ [0000-0002-2747-8894]

§ These authors contributed equally

[1]Centre for Chronobiology, Psychiatric Hospital of the University of Basel, Basel, Switzerland

[2]Research Platform Molecular and Cognitive Neurosciences, University of Basel, Basel, Switzerland

[3]Department of Biomedicine, University of Basel, Basel, Switzerland

[4]Consciousness and Cognition Lab, Department of Psychology, University of Cambridge, Cambridge, United Kingdom

[5]Translational Sensory and Circadian Neuroscience, Max Planck Institute for Biological Cybernetics, Tübingen, Germany

[6]TUM Department of Sport and Health Sciences (TUM SG), Technical University of Munich, Munich, Germany

[7]Psychiatric Hospital of the University of Basel, Basel, Switzerland

[8]Faculty of Health Sciences, Universidad Catolica del Maule, Talca, Chile

Corresponding Author:

Dr. Christine Blume

Centre for Chronobiology

Psychiatric Hospital of the University of Basel

Wilhelm-Klein-Str. 27

CH-4002 Basel, Switzerland

Email: christine.blume@unibas.ch

Authors' email addresses:

marinadphn@gmail.com

mn473@cam.ac.uk

manuel.spitschan@tum.de

martin.meyer@upk.ch

christian.cajochen@upk.ch

tb419@cam.ac.uk

afc37@cam.ac.uk

Abstract

During sleep, the human brain transitions to a 'sentinel processing mode', enabling the continued processing of environmental stimuli despite the absence of consciousness. Going beyond prior research, we employed advanced information-theoretic analyses, including mutual information (MI) and co-information (co-I), alongside event-related potential (ERP) and temporal generalization analyses (TGA), to characterize auditory prediction error processing across wakefulness and sleep. We hypothesized that a shared neural code would be present across sleep stages, with deeper sleep being associated with reduced information content and increased information redundancy.

To investigate this, twenty-nine young healthy participants were exposed to an auditory 'local-global' oddball paradigm during wakefulness and continued during an 8-hour sleep opportunity monitored via polysomnography. We focused on 'local' mismatch responses to a deviating fifth tone following four standard tones.

ERP analyses showed that prediction error processing continued throughout all sleep stages (N1-N3, REM). Mutual information analyses revealed a substantial reduction in the amount of encoded prediction error information during sleep, although ERP amplitudes increased with deeper NREM sleep. In addition, co-information analyses showed that neural dynamics became increasingly redundant with increasing sleep depth. Temporal generalisation analyses revealed a largely shared neural code between N2 and N3 sleep, although it differed between wakefulness and sleep.

Here, we showed how the neural code of the 'sentinel processing mode' changes from wake to light to deep sleep and REM, characterised by more redundant and less rich neural information in the human cortex as consciousness wanes. This altered stimulus processing reveals how neural information changes with the changes of consciousness states as we traverse the night.

Keywords: sleep, sensory processing, oddball, prediction error, information decomposition, consciousness

Introduction

Cognitive neuroscientists have extensively studied how cognitive processing persists during human sleep and what changes traverses from wakefulness to sleep. Convergent evidence suggests that even during behavioural unresponsiveness or unconsciousness, external stimuli are still processed although the 'cognitive code' may well have changed (Wielek et al., 2021). Event-related potentials (ERP) have helped characterise information processing during sleep (Andrillon et al., 2016; Blume et al., 2018; Blume et al., 2017; Oswald et al., 1960; Perrin et al., 1999), leading to the hypothesis that the brain enters a 'sentinel processing mode' during sleep (Blume et al., 2016; Blume et al., 2018; Legendre et al., 2019) where still relates to the environment and modulates behaviour accordingly. Strauss et al. (2015). A variant of an auditory oddball paradigm, first proposed by Bekinschtein et al. (2009), showed decreasing activity in the EEG activity with sleep stages (Strauss et al. (2015). Here we use a robust version of this task (cf. Figure 1 B) where the relevance of stimuli is solely determined by their (i) relative frequency of occurrence as well as their (ii) embedding in the context of other stimuli. This way, the task allows to investigate two levels of auditory (ir-)regularity detection: short-term (also termed 'local') and long-term (also termed 'global') (ir-)regularities. This manuscript focuses on violations of the short-term or 'local' irregularities resulting in low-level prediction errors. They become visible in the ERP as a mismatch negativity during wakefulness (Chennu & Bekinschtein, 2012; for a review see Näätänen et al., 2007; Näätänen et al., 1993; Sams et al., 1983).

In contrast, long-term or 'global' irregularities in turn manifest as a P300 response (Picton, 1992) during wakefulness with the response representing a high-level prediction error that requires attention (Chennu et al., 2013). From a nap study, Strauss et al. (2015) reported that while long-term prediction errors disappeared completely, short-term prediction errors were substantially modified during light sleep (stages N1 and N2) and REM sleep (note that deep sleep was not investigated). They concluded that auditory predictive processing at both levels of complexity was disrupted when behavioural responsiveness and consciousness was lost. We have recently investigated 'local' effects during a full night of sleep where, in contrast to Strauss et al., we found that a mismatch response indicating a short-term prediction error persists during all sleep stages (Blume et al., 2022). This suggests that at least low-level predictive abilities are not completely disrupted by a loss of consciousness during

sleep. More precisely, although the ERP waveform during sleep differed markedly from the one during wakefulness, the response appeared rather stereotypical, with the amplitude increasing concomitantly with increasing sleep depth during NREM, while the response during REM was similar to the N1 sleep response. The drawback of focusing on ERP or time-frequency direct signal analyses is that qualitative comparison of the sensory processing is confounded by their vigilance states. This is because the underlying brain activity is inherently different. Here, we therefore go beyond and applied temporal generalisation analyse (TGA) and Information Theory measures specifically developed for neural dynamics (Gelens et al., 2024; Ince et al., 2017). When TGA is applied within the same vigilance state (i.e., wakefulness, N1, etc.), it helps characterising the temporal organisation of information processing. When applied across vigilance states, i.e., when a classifier is for instance trained on wakefulness data and tested on data acquired during sleep, this method allows to evaluate to what extent the neural code is shared between different consciousness stages.

However, also this approach has its limitations: whether a classifier generalises or not does not unveil the actual information content of the signal, but just the similarity of the underlying activity pattern across trials or vigilance states. Since even decoding well above chance level can result from highly redundant information, the extent to which these analyses inform perceptual processes is still limited. We address this in a third set of analyses where we computed mutual information (MI) and co-information (co-I) to 'local' (ir-)regularities in different sleep stages. MI is an Information Theory measure capturing how much information about, in this case, a prediction error is contained in the neuronal signal. MI is quantified in normalized units of bits, representing an effect size unit that can be directly compared between vigilance stages (Ince et al., 2017). We further investigated whether the information about prediction error is redundant or synergistic across time. Redundancy across time means that, within a given electrode or region of interested, we observe the same trial-by-trial information between two different time points. Conversely, when the processing is synergistic, the combined time points convey more information about the prediction error than their sum (Gelens et al., 2024; Ince et al., 2017).

We expected temporal generalisation analyses (TGA) within and across vigilance stages to generalise for 'local' effects. This is because a mismatch response, like the local, seems partially

resistant to changes in the vigilance state (Garrido et al., 2009), which may be interpreted as a similar neural code being used. Regarding MI and co-I, we expected that less information about the prediction error would be encoded, particularly during NREM sleep, and that signals would become increasingly redundant with NREM sleep depth. During REM, we expected signal redundancy to decrease compared to NREM sleep and MI to increase. This is motivated by findings suggesting that EEG signal complexity is closest to wakefulness during REM sleep, with deep NREM sleep being associated with lowest complexity, and light NREM sleep with intermediate levels (Andrillon et al., 2016; Schartner et al., 2017).

Methods and Materials

Pre-registration

This study was pre-registered on Open Science Framework (OSF) including details about and code for the acoustic stimulation paradigm (https://osf.io/m23eh/?view_only=6b54a4756679459ab05bcf2215119f0d). We had also pre-registered the analytic strategy for EEG data preprocessing and ERP as well as temporal generalisation analyses. As the protocol was classified as a clinical study in Switzerland, it has also been registered on the German Clinical Trials Register (DRKS00023602).

Associated publications

Complementary data from this project have been presented in a previous manuscript (Blume et al., 2022), where we present in detail the effects of the two light conditions used on subjective sleepiness, behavioural vigilance, PSG-assessed sleep, subjective sleep quality, melatonin suppression, and local ERP effects in the local-global paradigm.

Participants

Following screening procedures, 40 volunteers had been invited to participate in the study between April 2019 and May 2020 (break: mid-March until May 2020 due to the Coronavirus pandemic). Prior to study inclusion, all participants provided written informed consent. Ten volunteers either dropped out or were excluded after the adaptation night or the first experimental night because

they did not adhere to elements of the study protocol. Thus, the final study sample comprised 30 volunteers (15 women). As melatonin analyses, which were relevant for the data analyses in Blume et al. (2022), did not yield valid data for one participant, the final sample comprised 29 participants (15 women). All volunteers were native German speakers (or comparable level) and scored in the normal range on questionnaires screening for sleep (Pittsburgh Sleep Quality Index [PSQI], inclusion if sum values ≤ 5; Buysse et al., 1989) and psychiatric disorders (Brief Symptom Inventory [BSI]; sum scores on nine subscales and 'global severity index' outside clinical range; Franke & Derogatis, 2000). Furthermore, they slept between 6 and 10 hours per night on workdays. Extreme chronotypes according to the Munich Chronotype Questionnaire (MCTQ; Roenneberg et al., 2003) were excluded. Self-selected HBT was on average 11:05 pm (range 10:15 pm – 00:00). Participants further had to be right-handed and between 18 and 30 years of age (M = 23.2±2.8 years; range 19-29 years). They did not report any vision or hearing problems and had normal or corrected-to-normal vision. If they wore glasses, these did not have a blue light filter. Volunteers were generally healthy non-smokers with a body-mass-index (BMI) between 18.6 and 24.9 (i.e., normal weight). Upon every arrival to the lab, volunteers had to take a urine-based multi-drug panel (nal von Minden GmbH, Germany) screening for amphetamines, tetrahydrocannabinol (THC), cocaine, benzodiazepines, morphine, and methadone. They were additionally seen by a study physician who again screened for exclusion criteria. Additional exclusion criteria were shift-work within the three months or travelling across >2 time zones in the month prior to study participation. The study protocol was approved by the ethics commission (Ethikkommission Nordwest- und Zentralschweiz; 2018-02003). Upon completion of the protocol participants received a remuneration of CHF 450.

Study procedures

The experimental protocol consisted of an adaptation night and two experimental visits to the lab, which were interspaced by two ambulatory study parts (cf. Figure 1). During the adaptation night, volunteers slept in the sleep laboratory at the Centre for Chronobiology in Basel in their pre-defined habitual sleep window (8-h sleep opportunity) with full polysomnography setup (for details see below). This was to familiarise them with the laboratory environment and to screen for previously undiscovered sleep disorders. To this end, sleep was evaluated informally regarding sleep onset latency, sleep

architecture, sleep efficiency, respiratory events as well as periodic limb movements. Following the adaptation night, they adhered to a pre-defined sleep-wake cycle for the next 7 days, which was verified using wrist actigraphy (ActiGraph LL.C, Pensacola, FL 32502, USA) and sleep logs. In more detail, they had to switch off lights ±30 min to the agreed [HBT] and get up ±30 min to habitual wake time. At the same time, they had to maintain an 8:16 h wake-sleep rhythm. In one case, the onset of the sleep opportunity was delayed by 30 minutes at the second visit, because the participant had consistently gone to bed at the end of the time window for lights off during the week preceding the lab visit. In another case, sleep was delayed due to technical failure of the display used for light exposure. The first experimental visit (see below) took place one week after the adaptation night. Following the first experimental visit, they again underwent the ambulatory protocol again before coming to the laboratory for a second and final visit.

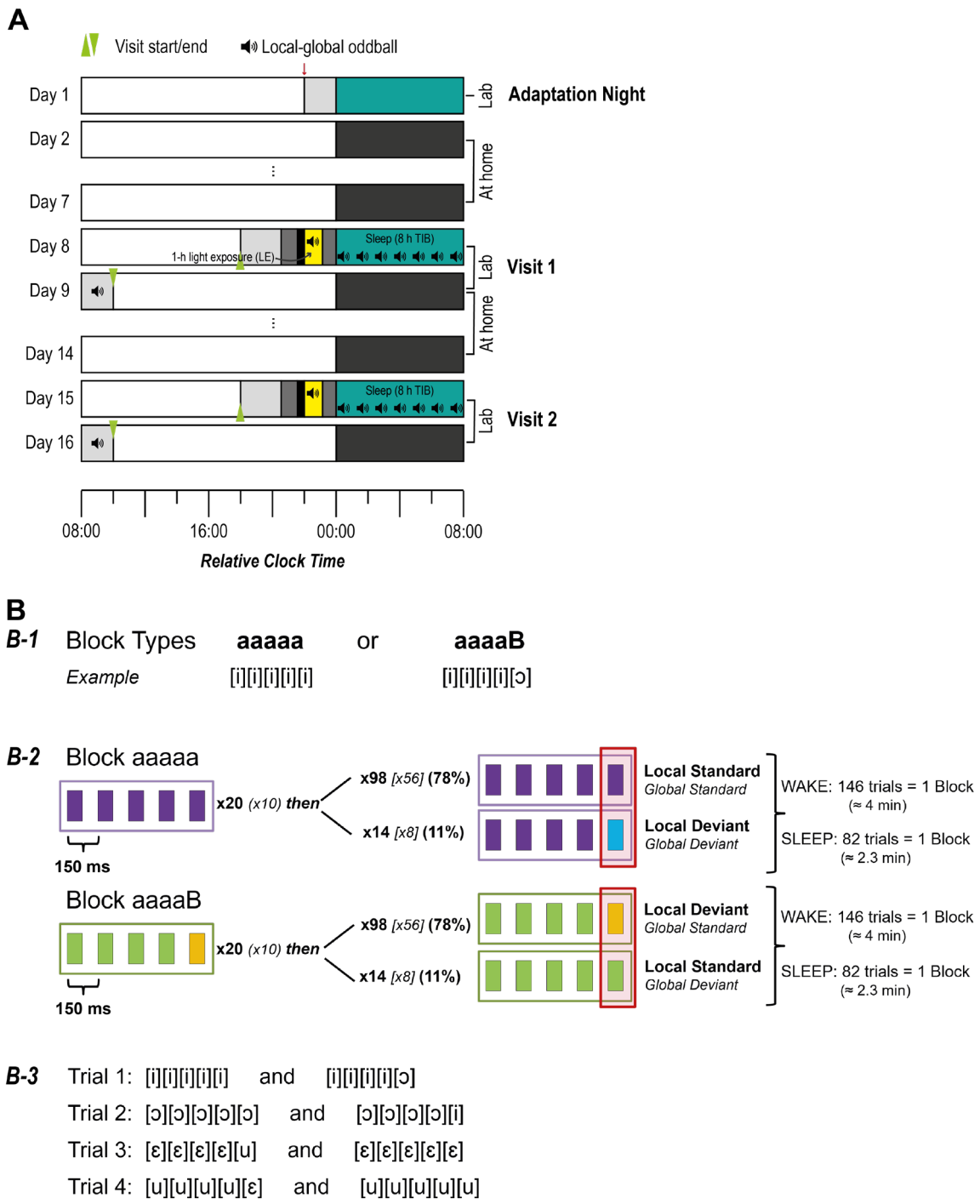

Figure 1. **(A)** ***Experimental protocol*** *for an exemplary participant (habitual bedtime [HBT] at 00:00). Following an adaptation night, participants came to the lab for two experimental visits, which were separated by one week and took place on the same day of the week. For the week prior to each experimental visit volunteers adhered to a circadian stabilisation protocol including fixed bed and wake times and 8 hours time in bed. Upon each experimental visit, participants arrived at the laboratory 5h 15min before their HBT or, at the latest, at 5:45 pm. From 1h 50 min before until 50 min before HBT they were exposed to one of two artificial light exposure conditions at each visit. The order of the light exposure conditions was counter-balanced across participants and sexes and here, we only used data from one of the visits (cf. main text). During the light exposure, during the night (8-hour sleep opportunity), as well as in the following morning, participants were exposed to the local-global oddball paradigm. The red arrow marks the point of final inclusion into the study.* ***(B) Local-Global Oddball Paradigm. (B-1)*** *Two different block types, i.e. "aaaaa" or "aaaaB", could serve as the standard block.* ***(B-2)*** *Upper panel: Following a habituation phase, participants were presented with local and/or global standards and deviants or omissions (not shown here). In a sequence of five stimuli the fifth stimulus could be a local standard (78%), a local deviant (11%), or an omission (11%; not shown here as they are outside the scope of this manuscript). In a global standard block, the sequence of five tones was identical to the standard sequence, whereas in a global deviant block, the sequence of five tones differed from the standard sequence. Lower panel: the global standard can also be an "aaaaB" block. In a sequence of five stimuli the fifth*

stimulus could be a local deviant (78%), a local standard (11%), or an omission (11%; not shown here). ***(B-3)*** *Example for four blocks used for a wakefulness recording. In blocks 1+2 an "aaaaa" sequence is the standard, in blocks 3+4 an "aaaaB" sequence. The local deviant vowels in blocks 1+3 become standard vowels in blocks 2+4. Adapted from Blume et al. (2022).*

Experimental nights took place on the same day of the week (i.e., Monday to Friday) with usually exactly one week in between the two visits. In three cases, the two experimental visits were spaced by a longer period up to 15 days (i.e., 11, 14, and 15 days) due to unforeseen circumstances. In two of these cases, the experimental visits took place on a different day of the week. Only in one case, the two experimental visits were spaced by 62 days, because of the lab being closed during the first wave of the Coronavirus pandemic in early 2020. Between the two experimental light exposure conditions, there were no condition differences in sleep measures, behavioural vigilance or subjective sleepiness nor differences in any of the ERP (cf. Blume et al., 2022) or TGA analyses. Differences were limited to stronger melatonin suppression (14%) in one of the light conditions (i.e., 'high-melanopic' light; for details on the light exposure conditions see Blume et al., 2022), which however were limited to the duration of the light exposure and not evident any longer when participants went to bed. Thus, we decided to limit the analyses for the present manuscript to the 'high-melanopic' condition. We aimed at counter-balancing the order of the light exposure conditions across participants and gender subgroups. However, drop-outs precluded counterbalancing among gender subgroups, wherefore the high-melanopic condition was the first for 8 men and 6 women.

Experimental visits

For the two experimental visits volunteers came to the lab 5 h 15 min before HBT or at 5:45 pm at the latest. The visits only differed regarding the light exposure conditions. However, as pointed out above, for this publication, we only used data from the high-melanopic condition. Upon arrival, they were served a sandwich and seated in a chair facing the display used for light exposure (still switched off at this time). Please note that we also regularly collected saliva samples for melatonin measurements and participants repeatedly completed assessments of psychomotor vigilance, rated their subjective sleepiness, and performed resting state EEG recordings in the evenings as well as after wake-up. These data are outside of the focus of this publication and have partly been published elsewhere (Blume et al., 2022). We began placing the EEG 4h 20 min before HBT. From 3h 20min until 2h 20min prior to HBT volunteers spent one hour in dim light. They for instance listened to podcasts and had to keep their eyes

open. Subsequently, they spent 30 min in complete darkness still with open eyes (ensured by checking the EOG for blinks). Following the dark adaptation period, the dim light served as a background light for the remainder of the evening. During the following 60 min of light exposure, they completed the auditory local-global oddball task (see below for details, overall duration approx. 41 minutes without breaks). The task started approx. eight minutes into the light exposure after another resting-state EEG measurement. With lights off, the local-global oddball task continued without interruptions until just before wake-up. Importantly, participants were instructed to continue counting global deviants and omissions as during the wakefulness while falling asleep and during the night (i.e., the same instructions as during the wakefulness recording). Previous research has shown that volunteers can follow such instructions even during sleep (e.g., Andrillon et al., 2016; Kouider et al., 2014). In the morning, thirty minutes after wake-up, participants completed another wakefulness-round of the local-global oddball paradigm (data are outside the scope of this manuscript).

Acoustic stimulation – Local-global oddball paradigm

Recordings during wakefulness took place in the evening during light exposure as well as in the mornings (delayed effects). In this manuscript, we focussed on the evening recordings only. During wakefulness and sleep, participants received instructions regarding the 'global' deviants, but not the 'local' deviants. Specifically, they were asked to count the number of deviants within a block.

More precisely, we adopted the design which Strauss et al. (2015, cf. Figure 1B) have previously used in which participants hear sequences of (here: German) vowels (100 ms each) and added omission trials, in which no sound was presented (as did Chennu et al., 2016). Note that in the present manuscript, we focus on the local effects only, wherefore the terms 'standard' or 'deviant' always refer to 'local' effects unless specified otherwise. One vowel was defined as the standard and presented much more frequently than the other, deviant, vowel. Vowels that were presented in the same sequence were chosen to be distant regarding their location of articulation (for possible combinations see Fig. 1-B3). Each trial comprised five stimuli where four standard vowels could either be followed by another (local) standard (78% of the trials in "aaaaa" blocks, 11% of the trials in "aaaaB" blocks), a (local) deviant (78% in "aaaaB" and 11% in "aaaaa" blocks). A deviating fifth stimulus, that is, a deviation on the level of a trial 5 stimuli, is termed a (local) deviant. In addition to the local effects the paradigm also includes so-called

global effects that concern the pattern of a series of trials. Specifically, a global standard is a trial of five stimuli (either “aaaaa” or “aaaaB”) that was initially presented 20 times (10 times during sleep) but is not of relevance for this manuscript. Additionally, we included some ‘omission’ trials, where an expected stimulus at the end of a sequence was simply omitted. Omission trials however are likewise outside the scope of this manuscript. These 20 (sleep: 10) presentations were followed by another global standard in ≈78% of the cases and by a global deviant or omission trial in ≈11% (see Fig. 1-B2). Each block consisted of 146 (±1) trials (82 [±1] during sleep). Stimuli were separated by an interstimulus interval of 50 ms and each trial was separated by an interval jittered between 850-1150 ms in 50 ms steps with an average of average 1000 ms. Two of the possible vowel combinations (cf. Fig. 1-B3) were used in the evenings and two in the mornings. During sleep, participants first only heard the same vowel combinations as in the evening. After approx. 40 min, when participants were expected to have reached N2 sleep, we also included the other two vowel combinations. On average, participants needed 10 min to reach N2 sleep (range 0.5-32.5 min). Besides the ‘normal’ blocks, we also included control blocks in which participants heard only standard trials during the first half of the block, which was followed by only omission trials. During wakefulness, participants were presented with a total of eight ‘normal’ blocks and two control blocks (approx. 41 min without breaks, self-paced). During sleep, there were 140 ‘normal’ blocks and 52 control blocks. Blocks during sleep were separated by a standard 6-s inter-block-interval (IBI) to mark transitions between blocks. In total, the stimulation during sleep summed up to 7.7 h. For further details on the preparation of the stimulus material and stimulus delivery, please see Blume et al. (2022), published open access.

Data collection, reduction, and evaluation

Sleep staging

Sleep was scored semi-automatically by the Siesta Group GmbH (Vienna, Austria; Anderer et al., 2005; Anderer et al., 2010). To this end, we down-sampled data from electrodes F3, F4, C3, C4, O1, and O2 as well as the EMG and an electrooculogram as recommended by AASM guidelines (American Academy of Sleep Medicine & Iber, 2007) to 128 Hz and exported the data to European Data Format (EDF) without further preprocessing.

Electrophysiological data collection and reduction

We recorded the EEG signal (sampling rate 250 Hz) using a BrainProducts® (BrainProducts GmbH, Gilching, Germany) LiveAmp® device. Twenty-three scalp electrodes (Ag-AgCl) were electrodes placed to allow sampling from the whole scalp. Two goldcup electrodes were additionally placed on the mastoids (i.e., A1/A2) to allow for later offline re-referencing (Grass® goldcup). An additional vertical Ag-AgCl electrode was placed below the left eye. Two further EOG goldcup electrodes were placed below the outer canthus of the left and above the outer canthus of the right eye, respectively, and referenced online to an additional A1 electrode. Besides this, we recorded a II-lead ECG and EMG activity was recorded from two chin electrodes (all Ag-AgCl). All Ag-AgCl electrodes were included in an EasyCap® (Easycap GmbH, Woerthsee-Etterschlag, Germany) EEG cap. Impedances were kept below 5kΩ and checked several times throughout the recording.

The pre-processing pipeline followed the steps previously specified in Blume et al. (2022). Data were high-pass filtered at 0.5 Hz and we corrected only wakefulness data for eye movement artefacts (horizontal/ vertical) with an independent-component analysis (ICA) performed on all EEG and EOG electrodes. This was followed by manual artefact rejection and low-pass filtering of the data at 40 Hz. Blinks during nocturnal periods of wakefulness were we manually corrected if necessary. Finally, we rereferenced the data to digitally linked mastoids offline and thereby 'regained' the online-reference FCz in the data. Subsequently, we added information about the sleep stage in which a stimulus was presented. For the event-related analyses (i.e., event-related potentials [ERPs] and time-frequency analyses), we segmented the data into (overlapping) segments from -2000 to +2000 ms relative to stimulus onset. Segments from the habituation/start phase (i.e., the first 20 trials of a block during wakefulness and the first 10 during sleep) were excluded.

Level 1: ERP analyses

For analyses of event-related potentials (ERPs), all trials were baseline-corrected using a 600 ms interval from -600 to 0 ms relative to the onset of the fifth stimulus. Thus, the baseline spanned the time from the onset of the first to the onset of the last stimulus (or where it should have started in omission trials) in a sequence of five. This relatively long baseline is a requirement for the time-frequency analyses. For sleep trials, we additionally distinguished between trials presented in each of the four

different sleep stages (i.e., N1, N2, N3, and REM sleep). We then averaged across trials separately for the wakefulness recordings and different sleep stages. If necessary, the number of trials was balanced within participants before averaging (i.e., if the available number of trials was for instance lower for deviants than for standards, we randomly selected a number of standard trials to match the number of deviant trials). For ERP effects, we considered the time window between the onset of the fifth stimulus and 900 ms. We performed EEG analyses in Matlab 2019a (The Mathworks, Natick, MA) using the Fieldtrip toolbox (Oostenveld et al., 2010) in the version distributed by the Salzburg Brain Dynamics lab (download date: 31-05-2019). For further details on EEG data pre-processing, please see Blume et al. (2022).

The statistical evaluation of ERPs was accomplished in Fieldtrip® using cluster-based permutation tests (Maris & Oostenveld, 2007). This is a data-driven approach which allows circumventing the problem of multiple comparisons in the presence of multiple time points/windows, electrodes, and possibly frequencies. Note that the local ERP effects had been included in a previous publication Blume et al. (2022), but are shown here for the purpose of completeness. For these comparisons, statistical analyses were followed-up by a visual inspection of all ERP waveforms to ascertain the validity of the effects. ERP and time-frequency analyses were one-sided with the critical alpha being set to 0.05. If reliable interactions were followed up with additional tests, we adjusted *p*-values for multiple comparisons using the method by Benjamini and Hochberg (1995).

Level 2: Temporal generalisation analyses

For the temporal generalisation analyses (TGA), we used the ADAM toolbox (Fahrenfort et al., 2018) for Matlab (The Mathworks, Natick, MA). The analytic procedure has been described in an easy-to-follow step-by-step fashion by Fahrenfort et al. (2018), wherefore we only include a concise overview here. First, we limited the data to a time window from -600 to 900 ms relative to stimulus onset. Subsequently, we ran the first-level analyses on the single-subject level focusing on the main effects, that is, the local and the global effects. We chose the backward decoding model; the input was raw data including all channels. A 10-fold cross validation was used, and data were down-sampled to 50 Hz. The 600 ms before stimulus onset served as the baseline interval, just as for the ERP analyses. The 'Area Under the Curve' (AUC; Bradley, 1997) served as the performance measure. Note that ADAM

automatically rebalances designs in case the trial counts in different cells of the factorial design differ (for instance, if there are more standard than deviant trials). In a second step, we then calculated the group level analyses within and across vigilance stages using the 'adam_compute_group_MVPA' function. We focussed on a time window from 200 ms before until 900 ms after stimulus onset and used the False Discovery Rate (Benjamini & Yekutieli, 2001) to control for multiple comparisons. The results were plotted using the function implemented in ADAM.

Level 3: Mutual Information and Co-Information analyses

Mutual Information (MI) and Co-information (co-I) analyses were computed on single-trial data for each vigilance state (i.e., wakefulness, N1-N3 sleep, REM sleep). The data basis was the same as for the temporal generalisation analyses, i.e. data had been down sampled to 50 Hz. The preprocessing was the same as for the ERP analyses. Using the GCMI toolbox (Ince et al., 2017), we averaged the signal across electrodes that were part of the reliable ERP clusters and quantified MI and co-I at each point in time. In information theory, Mutual Information (MI) quantifies the strength of the dependence (i.e., linear or non-linear) between two signals, and represents the information encoded by a pair of (neuronal) signals about the stimuli contrast, in this case standards and deviants. MI was computed between the stimulus class (i.e. standard, deviant) and the corresponding ERP signal. It reflects the normalised difference in entropy or effect size (unit: bits), i.e., the variability of a distribution independent of the underlying distribution, at every time point (for a detailed explanation see Ince et al., 2017). Due to the normalisation underlying its computation, MI can directly be compared across sleep stages, where large (small) MI corresponds to large (small) differences in entropy or effect size between standards and deviants. More precisely, 0.5 bits corresponds to a situation where two trials are sufficient to distinguish a standard from a deviant response. Additionally, on the basis of MI, we also computed co-I on a trial-by-trial basis. Importantly, co-I, which corresponds to a generalisation of MI to other time points, provides an advantage over decoding such as TGA alone. Specifically, techniques such as cross-decoding can only compute the predictive value of a multivariate pattern learned in one condition (e.g., wake) when tested on another condition (e.g., N2 sleep; cf. Figure 3), but they cannot specify whether the cross-decoded *information* is the same or not between conditions. In contrast, co-I captures both the redundant (or common; reflected by positive co-I values) information that a set of signals encodes about

a stimulus variable on trial-by-trial basis, and the synergistic (or extra; reflected by negative co-I values) information that a set of signals encode as a whole, above and beyond the information encoded by the sum of the isolated signals (Gelens et al., 2024; Ince et al., 2017). In the present analyses, positive co-I indicates that signals elicited at time points T1 and T2 contain redundant or overlapping information about the presented stimuli whereas negative co-I indicates that the information both signals is larger than when each signal is considered separately. Co-information (co-I) was calculated using the following formula:

$$\text{Co-I}(T1; T2; S) = I(T1; S) + I(T2; S) - I(T1, T2; S)$$

More precisely, I(T1; S) and I(T2; S) correspond to the mutual information (MI) between the signal at time points T1 and T2 for stimulus S (here: the difference between standard and deviant) at each point in time of the signal. I(T1, T2; S) corresponds to the MI between stimulus S and the combined signals from T1 and T2.

To test for reliable differences in co-I between pairs of vigilance stages, we used cluster-based permutation tests implemented in FieldTrip as in the ERP analyses (Maris & Oostenveld, 2007). In brief, co-I charts from pairs of vigilance stages (e.g., wakefulness vs. N1, cf. 5B) were compared. For each such pairwise comparison, trials in each condition were averaged within subjects. These averages were passed to the analysis procedure in FieldTrip, the details of which have been described previously (Maris & Oostenveld, 2007; also see ERP analyses). In short, this procedure compared corresponding temporal points in the subject-wise averages using independent samples *t*-tests for between-subject comparisons. Although this step was parametric, FieldTrip uses a nonparametric clustering method to address the multiple-comparisons problem. Here, the *t*-values of adjacent temporal points whose *p*-values are <0.05 are clustered together by summating their *t*-values, and the largest resulting cluster is retained. This procedure (i.e., the calculation of *t*-values at each point in time followed by clustering of adjacent *t*-values) was repeated 1000 times, with recombination and randomized resampling of the subject-wise averages before each repetition. This Monte Carlo method generates a nonparametric estimate of the *p*-value representing the statistical significance of the identified cluster. The cluster-level *t*-value was calculated as the sum of the individual *t*-values at the points within the cluster.

Results

Please note that results of the comprehensive analyses of melatonin secretion, subjective sleepiness, behavioural vigilance, subjective sleep quality, sleep parameters, and visual comfort ratings are published in Blume and collaborators (Blume et al., 2022). In short, there were no reliable condition differences between the two light exposure conditions on any parameter but melatonin (stronger suppression by high-melanopic than low-melanopic light, average difference 14%) that was limited to the duration of the light exposure. Thus, results presented here are always the data from the high-melanopic condition.

Sleep descriptives and sleep macrostructure

Note that data on objectively assessed sleep have previously been published in Blume et al. (2022), but are presented here again for the readers' convenience. The sleep characteristics presented in Table 1 confirm that all participants were healthy sleepers and sleep was not fundamentally altered by the auditory stimulation.

[Please insert Table 1 about here]

Table 1. Overview of the median and 95% confidence intervals of for latency to 10 min of continuous sleep, latency to N2, N3, and REM, percentage of N1, N2, N3, REM sleep, and wakefulness, sleep efficiency, wake after sleep onset (WASO), the total number of awakenings, and the arousal index (i.e., number of arousals per hour of total sleep time). Adapted from Blume et al. (2022).

Sleep parameter	
Latency to 10 min of continuous sleep (min)	7.0 (5.5-12.5)
Latency to N2 (min)	10.5 (7.5-12.5)
Latency to N3 (min)	21.5 (19.5-25.5)
Latency to REM (min)	144.5 (91.0-160.0)
N1 %	14.2 (11.7-16.5)
N2 %	40.2 (37.6-42.4)
N3 %	25.9 (23.4-30.4)
REM %	18.4 (16.4-22.7)
Sleep Efficiency (%)	94.1 (92.3-96.3)
Wake after sleep onset (WASO, min)	21.0 (13.5-31.5)
Number of awakenings	15 (11-19)
Arousal index (per h of total sleep time)	42.6 (18.0-52.5)

Level 1 - Event-related potentials (ERPs) local effects change in every sleep stage

The event-related potential responses for the local mismatch effect have likewise been presented in this earlier publication (Blume et al., 2022). As they form the basis of the level 2 (temporal

generalisation) and 3 (mutual information and co-information) analyses presented below, we will summarise them here again for convenience.

Generally, we found a reliable local mismatch effect during wakefulness and all sleep stages (i.e., N1, N2, N3, REM) with the waveform substantially changing from wakefulness to sleep (cf. Figure 3). In addition, as the depth of sleep increased, that is, from N1 to N3, the amplitudes increased, possibly due to the shift in power between bands in the underlying EEG, and the response became more spread out in time (cf. Figure 3 B-D). During REM, the mismatch response was similar to N1 (cf. Figure 3 B and E). For detailed statistical results, please see the supplementary material.

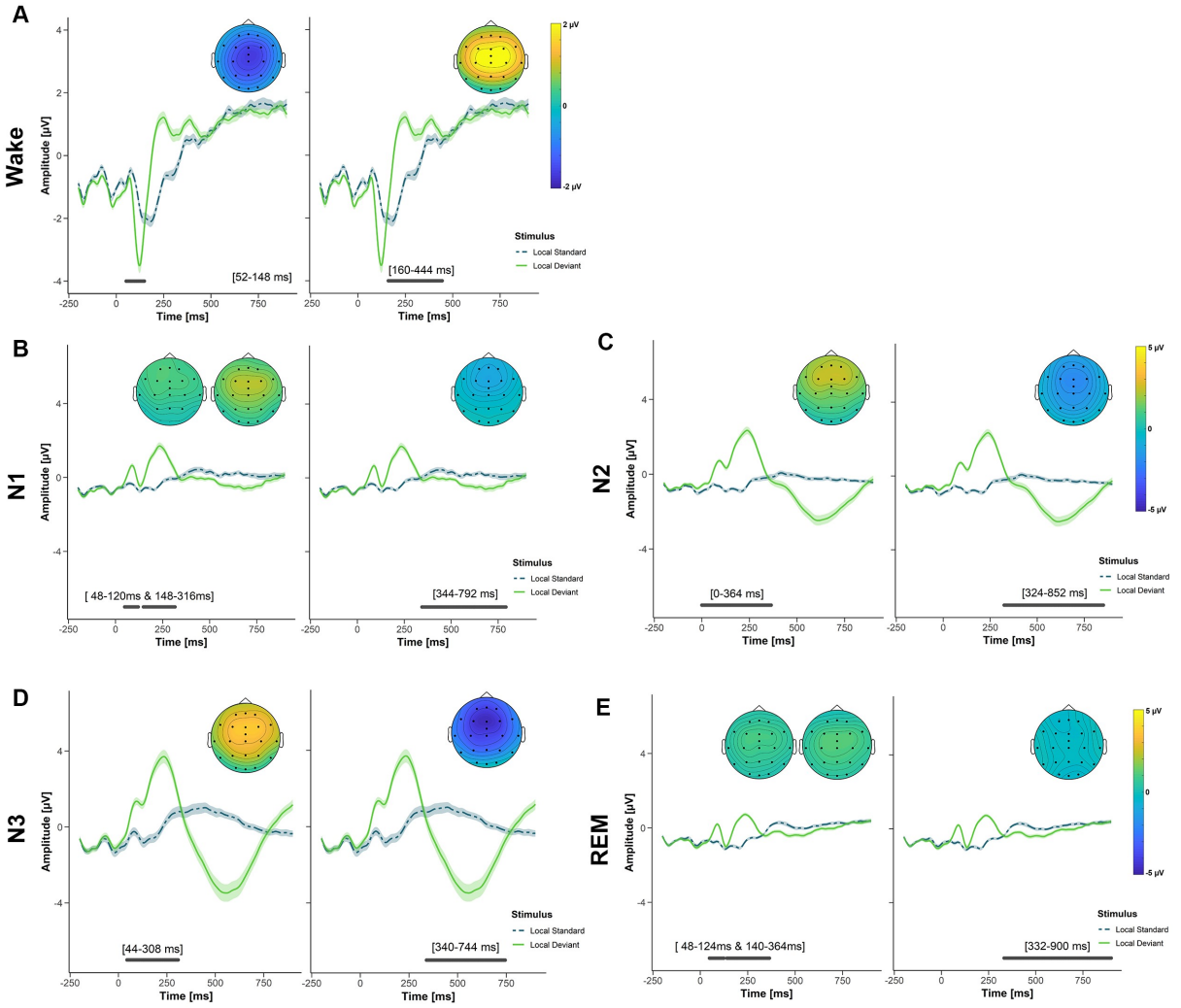

Figure 3: Event-related potential (ERP) elicited by deviants (green solid line) and standards (blue dashed line) effects during wakefulness (A), N1 (B), N2 (C), N3 (D), and REM (E) condition. The plots show the average ERP across all electrodes that were part of the reliable cluster, where the shaded area corresponds to the standard error. The electrodes that were part of the reliable cluster are indicated by black dots in the topoplots. The topoplots show the difference between the ERPs evoked by local deviants and standards. The reliable time windows are indicated by the grey horizontal bars included in each figure. Only reliable clusters are shown (cf. main text und supplementary material for more information). Adapted from Blume et al. (2022).

Level 2 - Temporal generalisation pattern generalise from N2 to N3 but not from awake to sleep stages

Next, we applied temporal generalisation analyses to learn more about the time course of the cognitive code and how information about the mismatch effect is propagated though the cortical hierarchy during wakefulness and different sleep stages (King & Dehaene, 2014). For the plots along the diagonal of Figure 4 (note that reliable clusters are circumscribed by solid red or blue lines; For the detailed statistical results, please see the supplementary material), a classifier was trained and tested on data from the same vigilance stage. The results indicate reliable decoding during wakefulness and all sleep stages, convergent with the univariate ERP results. Furthermore, the results show information about the mismatch is propagated though the cortical hierarchy across time in a rather chain-like response. There is a decrease in decoding accuracy across time points, which is particularly pronounced during wakefulness, where the peak in classification accuracy also is temporally well-aligned with the local mismatch response in the ERP (cf. Figure 2A). With increasing sleep depth, i.e., from N1 to N3, the classification accuracy becomes more jittered and spread out in time, which is also reminiscent of the ERP results (cf. Figure 2B-D). For the plots off the diagonal, the classifier was trained on a training dataset from one vigilance stage (e.g., wakefulness) and subsequently applied to a testing dataset from a different vigilance stage (e.g., N2 sleep) with the aim to identify similarities and differences in the cognitive code used in different vigilance stages. There was limited generalisation from wakefulness to sleep (or vice versa) while generalisation was especially strong between N2 and N3. While these analyses inform about the predictive value of a multivariate pattern learned in one vigilance state when tested in a different state, they are 'blind' to the actual information. This is, they cannot specify whether the cross-decoded information is the same or not between vigilance stages and whether the information is redundant or synergistic. Therefore, we also computed mutual information and co-information in a final analysis step.

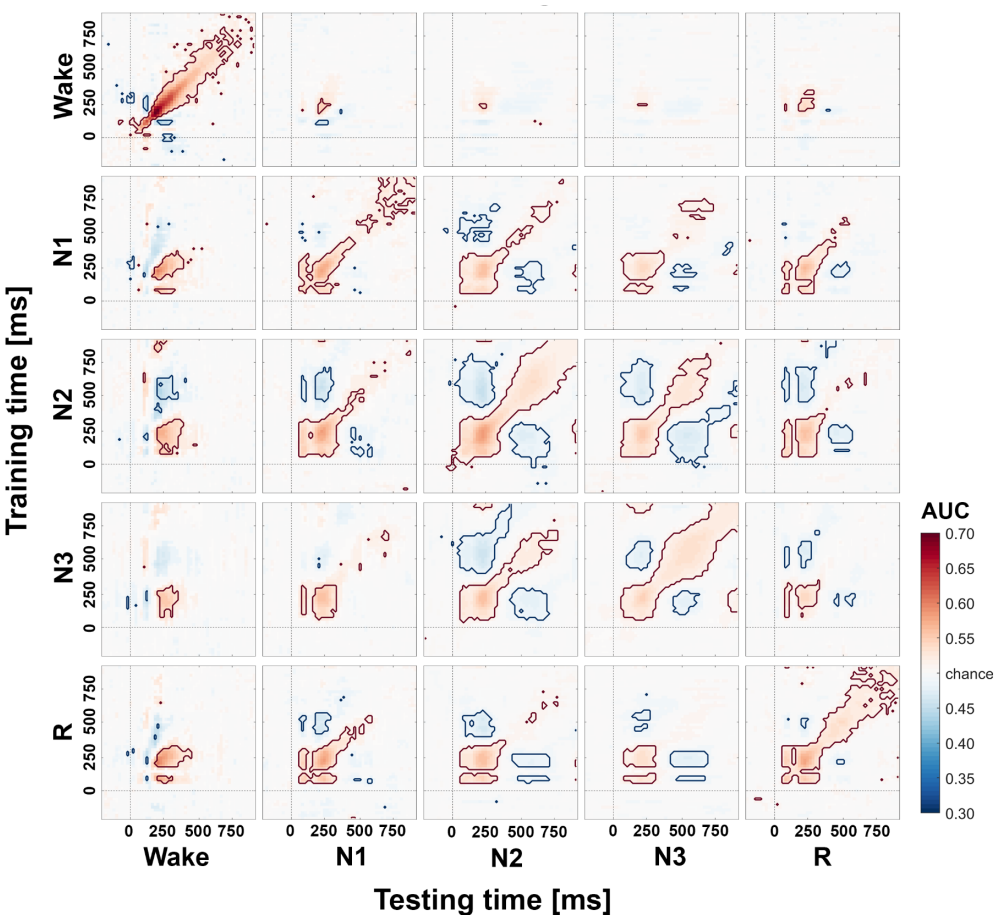

Figure 4: Temporal generalisation matrices for the local mismatch effect. The plots show the degree to which a classifier trained on a given time point (y-axis) generalized to other time points (x-axis). Decoding performance was evaluated within vigilance stages (matrices along the diagonal; wake, N1, N2, N3, and REM sleep) and across vigilance stages (matrices off the diagonal). The colour code represents low (cold colours) to high (warm colours) classification performance using the area under the curve (AUC). reliable clusters are circumscribed by solid red or blue lines. Note that below-chance classification (here in blue) occurs due to a polarity reversal in the underlying event-related potential (ERP). reliable clusters before stimulus onset are spurious clusters, possibly due to the rather long baseline (cf. main text and supplementary material).

Level 3 - Mutual information decreases with sleep stage and co-information redundancy increases

Finally, we aimed at directly quantifying the amount and type of information encoded about the local mismatch effect in the ERP signals (cf. Figure 2). First, we used MI to quantify the normalized effect size of the (local) mismatch effect that is visible in the ERPs. MI analyses revealed a higher effect size for wakefulness compared to all other vigilance stages (i.e., N1-N3 and REM; cf. Figure 5A, solid black traces). More precisely, MI averaged across 0-750 ms dropped from 0.0073 ± 0.001 bits (mean ± SEM) during wakefulness to 0.0036 ± 0.0006 bits during N1, 0.0052 ± 0.0006 bits during N2, 0.0042 ± 0.0007 bits during N3 and 0.0023 ± 0.0003 bits during REM; cf. Figure 5A). As expected, the peaks in MI were observed at latencies where ERP analyses had revealed reliable amplitude differences between deviant and standard tones (cf. Figure 2). Interestingly though, while there was temporal

convergence, the magnitude of the amplitude differences between ERPs were not proportional to the magnitude of the normalized effect sizes computed with MI (in bits). In fact, while the voltage amplitude differences in the ERPs tended to *increase* as a function of sleep depth (i.e., from N1 to N3) with amplitudes during REM being similar to N1, the normalized effect sizes (in bits) tend to *decrease* when computed with MI as can be seen from a comparison between Figures 2 and 5A).

The MI decreasing effects size results raise the question of whether sleep stages can also modulate the *type* of information encoded about the local mismatch effect. Thus, we additionally computed co-I to gain insight into the trial-by-trial information type by quantifying redundancy (i.e., negative co-I values) and synergy (i.e., positive co-I values) across neural signals (Gelens et al., 2024). The co-I analyses showed both redundant and synergistic patterns of information across time, with a predominance of redundancy across sleep stages (Figure 5A, upper row). To isolate the dynamics of redundant information across sleep stages, we depicted positive co-I values separately (Figure 5A, lower row). By visual inspection, redundant information seems to extend over greater latencies as a function of sleep. Also, the synergistic parts seem to become spread out in time. Cluster-based permutation tests comparing co-I charts between vigilance stages confirmed this impression and revealed increased redundancy (depicted in magenta in Figure 5B) particularly during N2 and N3 sleep as compared to wakefulness and N1. The redundant time windows showed substantial overlap in time with the second peak in MI (cf. Figure 5A).

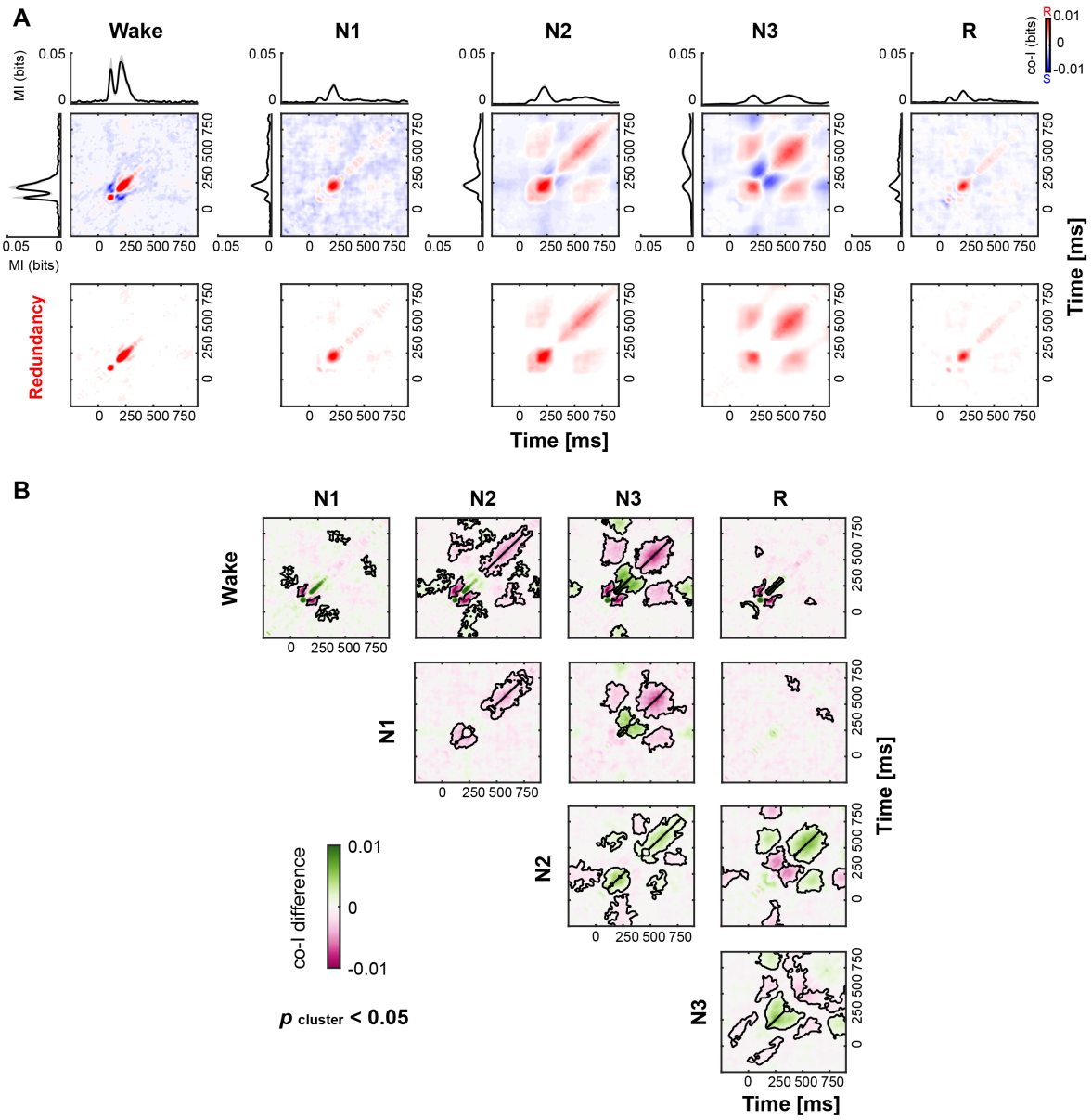

Figure 5: ***Co-Information: Temporal redundancy and synergy for the local mismatch effect. (A)*** *MI (black traces) between standard and deviant trials for wakefulness (0.0073 ± 0.001 bits; mean ± SEM, averaged across 0-750 ms), N1 (0.0036 ± 0.0006 bits), N2 (0.0052 ± 0.0006 bits) N3 (0.0042 ± 0.0007 bits), and REM sleep (0.0023 ± 0.0003 bits). The shaded gray area indicates SEM between participants. Temporal co-I was computed within ERP signals across time points. The average across participants is shown for the complete co-I chart (red/ blue panels); and for positive co-I values (i.e., redundancy only; red panel) for wake, N1-N3, and REM sleep.* ***(B)*** *Cluster-based permutation tests comparing co-I charts at the group level between pairs of vigilance stages (e.g. Wakefulness vs. N1). The plots show the degree to which a classifier trained on a given time point (y-axis) generalized to other time points (x-axis). Decoding performance was evaluated within vigilance stages (i.e., matrices along the diagonal; wakefulness, N1, N2, N3, and REM sleep) and across vigilance stages (i.e., matrices off the diagonal). The colour code represents differences in co-I between sleep stages (negative differences corresponding to higher redundancy in magenta; positive differences corresponding to higher synergy in green). Reliable clusters are circumscribed by black lines (p<0.05).*

Discussion

In this project, we used innovative information-theoretic analyses, i.e. mutual information (MI) and co-information (co-I) analyses, in addition to more classical event-related potential (ERP) and temporal generalisation (TGA) analyses, to investigate the brain's ability to generate expectations and respond to their violation across vigilance states (i.e. wakefulness, N1-N3, and REM sleep) in an auditory oddball task. In line with our hypotheses, mutual information (MI) analyses revealed a reduced ability of the brain to encode information about prediction error during sleep compared to wakefulness. Further, and for the first time, using co-I analyses we show, that the deeper the NREM sleep, the more redundant the processing became, with REM sleep being similar to N1. Deeper sleep was associated with less differentiated processing: the brain simply processed "more of the same information". This change in stimulus processing is reflected in the loss of consciousness we experience during sleep. In other words, the lower consciousness levels during sleep may be explained as informationally weaker and poor states regarding their external stimuli processing capabilities.

More specifically, during sleep MI, which expresses an effect size in bits and can therefore be directly compared across sleep stages (Ince et al., 2017), dropped from 0.0073 ± 0.001 bits (mean ± SEM; averaged across 0-750 ms) during wakefulness to an average of 0.0038 ± 0.0013 bits during sleep (cf. Figure 5A). This suggests that the difference in effect size between (local) standards and deviants in the auditory oddball paradigm was decreased during sleep (i.e., N1-N3 and REM sleep), or in simpler terms, that less information about the prediction error was encoded. This contrasts with the increase in amplitude when sleep became deeper (i.e., from N1 to N3) that we observed in the ERP analyses (cf. Figure 3), and shows that the amplitude of ERPs, or differences between them, is not a valid indicator of the amount of information processing taking place in the brain. Rather, the increased amplitudes reflect underlying shifts in the EEG power spectrum that are characteristic for different sleep stages. Going beyond the MI findings, co-I analyses yielded that especially redundant information extended over greater latencies during sleep compared to wakefulness, suggesting that (local) mismatch processing became less neurally differentiated during sleep. This effect was further modulated by sleep depth, with time windows of redundant information becoming more spread out from N1 to N3 sleep suggesting that the brain processed more of the same information across time (cf. Figure 5). Results

obtained during REM sleep were largely similar to N1. Importantly, the redundant time windows showed substantial overlap with the second peak observed in the MI results (cf. Figure 5; line plots). Interestingly, particularly during deep N3 sleep, also the synergistic parts seemed to become extended in time, suggesting further differences in the information processing of auditory deviance for deep sleep compared to light sleep, REM and wake. Overall, these findings complement the results obtained with temporal generalisation analyses (TGA), that is, multivariate classifiers, where cross-decoding likewise seemed to become extended in time. However, such classifiers are limited as they can only inform about the predictive value of a (multivariate) pattern learned in one condition (e.g., wakefulness) when applied to another condition (e.g., N2 sleep). Thus, they are essentially 'blind' to the actual cross-decoded information and cannot inform whether the decoded information is indeed the same or different in the two conditions – a gap that co-I fills. In the present analyses, TGA hardly showed generalisation from wakefulness to sleep and vice versa and only limited generalisation between N1 and REM on the one hand, and N2 and N3 sleep on the other hand. However, N2 and N3 sleep seemed to share a common neural signature of the processing of mismatch information. This is in line with earlier findings by Wielek et al. (2021) who reported that classifiers trained to distinguish responses elicited by stimuli varying in their salience (i.e., familiar vs. unfamiliar voice stimuli) generalised from N2 to N3 and vice versa, but not between wakefulness and sleep (i.e., N1-N3, REM).

Importantly, using information-theoretic analyses in addition to more classical ERP and TGA analyses also allowed us to go well beyond previous studies that had investigated prediction error processing during sleep. Strauss et al. (2015) also used a global-local paradigm during an afternoon nap and concluded that the processing of local (and global) mismatches is disrupted during sleep. In contrast, we found the local mismatch response to be clearly present during all sleep stages, modified but not disrupted (cf., Figure 2 and Blume et al., 2022). This may be due to the improved signal-to-noise ratio as Strauss and colleagues only had data from an afternoon nap. At the same time, our information-theoretic analyses revealed that processing during sleep was substantially altered showing a decrease in the amount of information about the prediction error encoded (cf. MI results) as well as a shift towards redundant processing that became sustained in time (cf. co-I results). From this perspective, MI and co-I analyses allowed us to further characterise the sentinel processing mode that the brain has been

suggested to enter during sleep (e.g., Blume et al., 2016; Blume et al., 2018; Legendre et al., 2019). More precisely, this mode allows the brain to continue processing external stimuli during sleep in lower states or absence of consciousness, while carefully balancing the need to stay asleep with the need to wake up, for instance in the case of danger. Previous studies found that salient acoustic stimuli, for instance one's own name (Blume et al., 2016; Perrin et al., 1999), angry prosody (Blume et al., 2016), an unfamiliar voice (Blume et al., 2018), and task-relevant stimuli (Kouider et al., 2014) elicited stronger brain signals such as higher amplitude ERPs compared to less salient stimuli (i.e., unfamiliar names, neutral prosody, familiar voice, task-irrelevant stimuli) during sleep. Legendre et al. (2019) concluded that the brain 'amplified' meaningful compared to irrelevant streams of speech, during N2 sleep but not during deep N3 sleep. Going beyond these findings, we here show that the 'sentinel processing mode' is characterised by i) less information encoded and ii) more redundant information processing, iii) that is further sustained in time as a function of sleep depth (i.e., from N1 to N3 sleep). Further, these characteristics may also explain why we lose conscious processing to external stimuli during sleep, that is, in the 'sentinel processing mode'. Previous research showed that during conscious wakefulness, the response to a transcranial magnetic stimulation (TMS) pulse initiates a long-range pattern of cortical activation (Massimini et al., 2009; Massimini et al., 2005; Sarasso et al., 2014). However, during N3 sleep, as well as general anaesthesia, such a TMS pulse gave rise to a stereotypical high-amplitude response, with a waveform echoing the ERPs we found here (cf. Figure 2; also see Arzi et al., 2021). Additionally, the response after the TMS pulse was rapidly extinguished and hardly propagated beyond the stimulation site, that is, it remained rather local in cortical space. During REM, the TMS-induced response became more complex again, indicating that effective connectivity among cortical areas partially recovered. The authors concluded that the loss of consciousness during NREM sleep was associated with a breakdown in cortical effective connectivity. In line with this, it has also been reported that EEG signal complexity is reduced during sleep (Andrillon et al., 2016; Schartner et al., 2017). We propose that the decrease in the amount of information encoded as well as the increased redundancy that became evident in the present analyses of violations of expectations at the 'local' level could be explained by this loss of effective connectivity observed using the TMS perturbational approach.

Here, we used MI and co-I analyses to investigate for the first time human predictive processes during sleep. While we focused on low-level or 'local' prediction errors, future studies should apply the same methods also to prediction errors at higher levels of complexity (i.e., 'global' mismatch responses, perceptual decision making) and investigate the extent to which stimulus processing is altered by the presence of for instance sleep spindles (Cote et al., 2000; Elton et al., 1997; Schabus et al., 2012), K-complexes (Ameen et al., 2022b), the slope of slow oscillations (Massimini et al., 2003; Schabus et al., 2012), or during tonic vs. phasic REM sleep (Price & Kremen, 1980; Sallinen et al., 1996; TAKAHARA et al., 2002; Wehrle et al., 2007).

To conclude, we show that processing of prediction errors in an auditory oddball paradigm during sleep was characterised by a decrease in the amount of information encoded as well as an increase in the redundancy of neuronal signals. Importantly, the degree of redundancy increased with NREM sleep depth, i.e. from N1 to N3 sleep, and redundant processing became more sustained in time, while REM was comparable to N1. Applying innovative information-theoretic analyses to human brain data during wakefulness and sleep allowed us to go well beyond previous research, which mostly focused on the analysis of ERPs or multivariate pattern classifiers such as temporal generalisation analyses (TGA). These more classic analyses revealed continued processing of the (local) mismatch response during all sleep stages, a shared neural signature particularly between prediction error processing in N2 and N3 sleep, but only to a very limited extent between wakefulness and sleep. Our approach allowed us to characterise the 'sentinel processing mode' the brain switches to during sleep (Ameen et al., 2022a; Blume et al., 2018; Legendre et al., 2019) in more depth than previous research. Finally, the identified processing characteristics also help understand why we lose consciousness when falling asleep as it shows the dynamics of neural information changes its differences between states.

Funding

The project was supported by the following grants awarded to CB: a fellowship of the Austrian Science Fund (FWF; J-4243), a grant from the Research Fund for Junior Researchers of the University of Basel, an Ambizione grant from the Swiss National Science Foundation (SNF; Project No. 201742), and funds from the Freiwillige Akademische Gesellschaft (FAG), the Novartis Foundation for Biological-Medical Research, and the Psychiatric Hospital of the University of Basel (UPK). ACJ is supported by an ANID/FONDECYT Regular (1240899) research grant.

Conflict of interest

Related to lighting, M.S. is currently an unpaid member of CIE Technical Committee TC 1–98 ('A Roadmap Toward Basing CIE Colorimetry on Cone Fundamentals'). M.S. was an unpaid advisor to the Division Reportership DR 6–45 of Division 3 ('Publication and maintenance of the CIE S026 Toolbox') and a member of the CIE Joint Technical Committee 9 on the definition of CIE S 026:2018. Since 2020, M.S. is an elected Member of the Daylight Academy and an unpaid member of the Board of Advisors of the Center for Environmental Therapeutics. C.C. has had the following commercial interests related to lighting: honoraria, travel, accommodation and/ or meals for invited keynote lectures, conference presentations or teaching from Toshiba Materials, Velux, Firalux, Lighting Europe, Electrosuisse, Novartis, Roche, Elite, Servier and WIR Bank. C.C. is an elected member of the Daylight Academy. C.B. has had the following commercial interests related to sleep and/or light: honoraria for invited talks and workshops from IKEA, F.A. Hoffmann-La Roche AG, L'Oréal, Swissline Cosmetics, and Vattenfall. C.B. is an elected member of the Daylight Academy. The remaining authors declare no competing interests.

Ethical approval

Ethical approval was provided by the cantonal ethics commission (Ethikommission Nordwest- und Zentralschweiz; 2018-02003). The study was conducted in accordance with Swiss law and the Declaration of Helsinki.

Acknowledgements

We thank all participants, who volunteered to participate in the project. We especially also thank the interns Anaité del Río, Patricia Egli, Corinna M. Hofer, Jessica Jacobs, Melina Koller, Daniela

Lindegger, Marlene Schmidt, and Natascha Stoffel without whom the study could not have been conducted. We also thank Robin A.A. Ince for his valuable support with the information-theoretic analyses and Lavazza for the continuous support.

References

Ameen, M. S., Heib, D. P., Blume, C., & Schabus, M. (2022a). The brain selectively tunes to unfamiliar voices during sleep. *Journal of Neuroscience*. https://doi.org/10.1523/JNEUROSCI.2524-20.2021

Ameen, M. S., Heib, D. P. J., Blume, C., & Schabus, M. (2022b). The Brain Selectively Tunes to Unfamiliar Voices during Sleep. *The Journal of Neuroscience*, *42*(9), 1791-1803. https://doi.org/10.1523/jneurosci.2524-20.2021

American Academy of Sleep Medicine, & Iber, C. (2007). *The AASM manual for the scoring of sleep and associated events: rules, terminology and technical specifications*. American Academy of Sleep Medicine.

Anderer, P., Gruber, G., Parapatics, S., Woertz, M., Miazhynskaia, T., Klösch, G., Saletu, B., Zeitlhofer, J., Barbanoj, M. J., & Danker-Hopfe, H. (2005). An E-health solution for automatic sleep classification according to Rechtschaffen and Kales: validation study of the Somnolyzer 24× 7 utilizing the Siesta database. *Neuropsychobiology*, *51*(3), 115-133.

Anderer, P., Moreau, A., Woertz, M., Ross, M., Gruber, G., Parapatics, S., Loretz, E., Heller, E., Schmidt, A., Boeck, M., Moser, D., Kloesch, G., Saletu, B., Saletu-Zyhlarz, G. M., Danker-Hopfe, H., Zeitlhofer, J., & Dorffner, G. (2010). Computer-Assisted Sleep Classification according to the Standard of the American Academy of Sleep Medicine: Validation Study of the AASM Version of the Somnolyzer 24 × 7. *Neuropsychobiology*, *62*(4), 250-264. https://www.karger.com/DOI/10.1159/000320864

Andrillon, T., Poulsen, A. T., Hansen, L. K., Léger, D., & Kouider, S. (2016). Neural Markers of Responsiveness to the Environment in Human Sleep. *The Journal of Neuroscience*, *36*(24), 6583-6596. https://doi.org/10.1523/jneurosci.0902-16.2016

Arzi, A., Trentin, C., Laudini, A., Krugliak, A., Nikolla, D., & Bekinschtein, T. (2021). Dynamic Auditory Remapping Across the Sleep-Wake Cycle. *bioRxiv*, 2021.2002.2016.431383. https://doi.org/10.1101/2021.02.16.431383

Bekinschtein, T. A., Dehaene, S., Rohaut, B., Tadel, F., Cohen, L., & Naccache, L. (2009). Neural signature of the conscious processing of auditory regularities. *Proceedings of the National Academy of Sciences*, *106*(5), 1672-1677. https://doi.org/10.1073/pnas.0809667106

Benjamini, Y., & Hochberg, Y. (1995). Controlling the False Discovery Rate: A Practical and Powerful Approach to Multiple Testing. *Journal of the Royal Statistical Society. Series B (Methodological)*, *57*(1), 289-300. https://doi.org/10.2307/2346101

Benjamini, Y., & Yekutieli, D. (2001). The control of the false discovery rate in multiple testing under dependency. *Annals of statistics*, 1165-1188.

Blume, C., del Giudice, R., Lechinger, J., Wislowska, M., Heib, D. P., Hoedlmoser, K., & Schabus, M. (2016). Preferential processing of emotionally and self-relevant stimuli persists in unconscious N2 sleep. *Brain and Language*. https://doi.org/10.1016/j.bandl.2016.02.004

Blume, C., del Giudice, R., Wislowska, M., Heib, D. P., & Schabus, M. (2018). Standing sentinel during human sleep: Continued evaluation of environmental stimuli in the absence of consciousness. *Neuroimage*, *178*, 638-648. https://doi.org/10.1016/j.neuroimage.2018.05.056

Blume, C., del Giudice, R., Wislowska, M., Heib, D. P. J., & Schabus, M. (2017). *Continued Evaluation of Stimulus Familiarity during Naturally Occurring Unconsciousness* 13th International Conference on Cognitive Neuroscience (ICON), Amsterdam, The Netherlands.

Blume, C., Niedernhuber, M., Spitschan, M., Slawik, H. C., Meyer, M. P., Bekinschtein, T. A., & Cajochen, C. (2022). Melatonin suppression does not automatically alter sleepiness, vigilance, sensory processing, or sleep. *Sleep*. https://doi.org/10.1093/sleep/zsac199

Bradley, A. P. (1997). The use of the area under the ROC curve in the evaluation of machine learning algorithms. *Pattern Recognition*, *30*(7), 1145-1159. https://doi.org/https://doi.org/10.1016/S0031-3203(96)00142-2

Buysse, D. J., Reynolds, C. F., Monk, T. H., Berman, S. R., & Kupfer, D. J. (1989). The Pittsburgh sleep quality index: A new instrument for psychiatric practice and research. *Psychiatry Research*, *28*(2), 193-213. https://doi.org/https://doi.org/10.1016/0165-1781(89)90047-4

Chennu, S., & Bekinschtein, T. A. (2012). Arousal modulates auditory attention and awareness: insights from sleep, sedation, and disorders of consciousness. *Attention and Consciousness in Different Senses*, 14.

Chennu, S., Noreika, V., Gueorguiev, D., Blenkmann, A., Kochen, S., Ibáñez, A., Owen, A. M., & Bekinschtein, T. A. (2013). Expectation and Attention in Hierarchical Auditory Prediction. *The Journal of Neuroscience*, *33*(27), 11194-11205. https://doi.org/10.1523/jneurosci.0114-13.2013

Chennu, S., Noreika, V., Gueorguiev, D., Shtyrov, Y., Bekinschtein, T. A., & Henson, R. (2016). Silent Expectations: Dynamic Causal Modeling of Cortical Prediction and Attention to Sounds That Weren't. *The Journal of Neuroscience*, *36*(32), 8305-8316. https://doi.org/10.1523/jneurosci.1125-16.2016

Cote, K. A., Epps, T. M., & Campbell, K. B. (2000). The role of the spindle in human information processing of high-intensity stimuli during sleep. *Journal of Sleep Research*, *9*(1), 19-26. https://doi.org/10.1046/j.1365-2869.2000.00188.x

Elton, M., Winter, O., Heslenfeld, D., Loewy, D., Campbell, K., & Kok, A. (1997). Event-related potentials to tones in the absence and presence of sleep spindles. *Journal of Sleep Research*, *6*(2), 78-83.

Fahrenfort, J. J., Van Driel, J., Van Gaal, S., & Olivers, C. N. (2018). From ERPs to MVPA using the Amsterdam decoding and modeling toolbox (ADAM). *Frontiers in Neuroscience*, *12*, 368.

Franke, G. H., & Derogatis, L. R. (2000). *BSI: Brief Symptom Inventory von LR Derogatis:(Kurzform der SCL-90-R): deutsche Version: Testmappe*. Beltz Test.

Garrido, M. I., Kilner, J. M., Stephan, K. E., & Friston, K. J. (2009). The mismatch negativity: A review of underlying mechanisms. *Clinical Neurophysiology*, *120*(3), 453-463. https://doi.org/https://doi.org/10.1016/j.clinph.2008.11.029

Gelens, F., Äijälä, J., Roberts, L., Komatsu, M., Uran, C., Jensen, M. A., Miller, K. J., Ince, R. A. A., Garagnani, M., Vinck, M., & Canales-Johnson, A. (2024). Distributed representations of prediction error signals across the cortical hierarchy are synergistic. *Nature Communications*, *15*(1), 3941. https://doi.org/10.1038/s41467-024-48329-7

Ince, R. A. A., Giordano, B. L., Kayser, C., Rousselet, G. A., Gross, J., & Schyns, P. G. (2017). A statistical framework for neuroimaging data analysis based on mutual information estimated via a gaussian copula. *Human Brain Mapping*, *38*(3), 1541-1573. https://doi.org/https://doi.org/10.1002/hbm.23471

King, J. R., & Dehaene, S. (2014). Characterizing the dynamics of mental representations: the temporal generalization method. *Trends in Cognitive Sciences*, *18*(4), 203-210. https://doi.org/10.1016/j.tics.2014.01.002

Kouider, S., Andrillon, T., Barbosa, Leonardo S., Goupil, L., & Bekinschtein, Tristan A. (2014). Inducing Task-Relevant Responses to Speech in the Sleeping Brain. *Current Biology*, *24*(18), 2208-2214. https://doi.org/http://dx.doi.org/10.1016/j.cub.2014.08.016

Legendre, G., Andrillon, T., Koroma, M., & Kouider, S. (2019). Sleepers track informative speech in a multitalker environment. *Nature Human Behaviour*, *3*(3), 274-283. https://doi.org/10.1038/s41562-018-0502-5

Maris, E., & Oostenveld, R. (2007). Nonparametric statistical testing of EEG-and MEG-data. *Journal of Neuroscience Methods*, *164*(1), 177-190.

Massimini, M., Boly, M., Casali, A., Rosanova, M., & Tononi, G. (2009). A perturbational approach for evaluating the brain's capacity for consciousness. In S. Laureys, N. D. Schiff, & A. M. Owen (Eds.), *Progress in Brain Research* (Vol. 177, pp. 201-214). Elsevier. https://doi.org/https://doi.org/10.1016/S0079-6123(09)17714-2

Massimini, M., Ferrarelli, F., Huber, R., Esser, S. K., Singh, H., & Tononi, G. (2005). Breakdown of Cortical Effective Connectivity During Sleep. *Science*, *309*(5744), 2228-2232. https://doi.org/doi:10.1126/science.1117256

Massimini, M., Rosanova, M., & Mariotti, M. (2003). EEG slow (~ 1 Hz) waves are associated with nonstationarity of thalamo-cortical sensory processing in the sleeping human. *Journal of neurophysiology*, *89*(3), 1205-1213.

Näätänen, R., Paavilainen, P., Rinne, T., & Alho, K. (2007). The mismatch negativity (MMN) in basic research of central auditory processing: a review. *Clin Neurophysiol*, *118*(12), 2544-2590. https://doi.org/10.1016/j.clinph.2007.04.026

Näätänen, R., Paavilainen, P., Tiitinen, H., Jiang, D., & Alho, K. (1993). Attention and mismatch negativity [Research Support, Non-U.S. Gov't]. *Psychophysiology*, *30*(5), 436-450. http://www.ncbi.nlm.nih.gov/pubmed/8416070

Oostenveld, R., Fries, P., Maris, E., & Schoffelen, J.-M. (2010). FieldTrip: open source software for advanced analysis of MEG, EEG, and invasive electrophysiological data. *Computational Intelligence and Neuroscience*, *2011*.

Oswald, I., Taylor, A. M., & Treisman, M. (1960). Discriminative responses to stimulation during human sleep. *Brain*.

Perrin, F., Garcia-Larrea, L., Mauguiere, F., & Bastuji, H. (1999). A differential brain response to the subject's own name persists during sleep. *Clinical Neurophysiology*, *110*(12), 2153-2164. http://www.ncbi.nlm.nih.gov/pubmed/10616121

Picton, T. W. (1992). The P300 wave of the human event-related potential. *Clinical Neurophysiology*, *9*(4), 456-479. http://ukpmc.ac.uk/abstract/MED/1464675

Price, L. J., & Kremen, I. (1980). Variations in Behavioral Response Threshold Within the REM Period of Human Sleep. *Psychophysiology*, *17*(2), 133-140. https://doi.org/https://doi.org/10.1111/j.1469-8986.1980.tb00125.x

Roenneberg, T., Wirz-Justice, A., & Merrow, M. (2003). Life between Clocks: Daily Temporal Patterns of Human Chronotypes. *Journal of Biological Rhythms*, *18*(1), 80-90. https://doi.org/10.1177/0748730402239679

Sallinen, M., Kaartinen, J., & Lyytinen, H. (1996). Processing of auditory stimuli during tonic and phasic periods of REM sleep as revealed by event-related brain potentials. *Journal of Sleep Research*, *5*(4), 220-228. https://doi.org/10.1111/j.1365-2869.1996.00220.x

Sams, M., Alho, K., & Näätänen, R. (1983). Sequential effects on the ERP in discriminating two stimuli. *Biol Psychol*, *17*(1), 41-58. https://doi.org/https://doi.org/10.1016/0301-0511(83)90065-0

Sarasso, S., Rosanova, M., Casali, A. G., Casarotto, S., Fecchio, M., Boly, M., Gosseries, O., Tononi, G., Laureys, S., & Massimini, M. (2014). Quantifying Cortical EEG Responses to TMS in (Un)consciousness. *Clinical EEG and Neuroscience*, *45*(1), 40-49. https://doi.org/10.1177/1550059413513723

Schabus, M., Dang-Vu, T. T., Heib, D. P. J., Boly, M., Desseilles, M., Vandewalle, G., Schmidt, C., Albouy, G., Darsaud, A., & Gais, S. (2012). The fate of incoming stimuli during NREM sleep is determined by spindles and the phase of the slow oscillation. *Frontiers in Neurology*, *3*.

Schartner, M. M., Pigorini, A., Gibbs, S. A., Arnulfo, G., Sarasso, S., Barnett, L., Nobili, L., Massimini, M., Seth, A. K., & Barrett, A. B. (2017). Global and local complexity of intracranial EEG decreases during NREM sleep. *Neuroscience of Consciousness*, *2017*(1). https://doi.org/10.1093/nc/niw022

Strauss, M., Sitt, J. D., King, J.-R., Elbaz, M., Azizi, L., Buiatti, M., Naccache, L., van Wassenhove, V., & Dehaene, S. (2015). Disruption of hierarchical predictive coding during sleep. *Proceedings of the National Academy of Sciences*, *112*(11), E1353-E1362.

TAKAHARA, M., NITTONO, H., & HORI, T. (2002). Comparison of the event-related potentials between tonic and phasic periods of rapid eye movement sleep. *Psychiatry and Clinical Neuroscience*, *56*(3), 257-258. https://doi.org/https://doi.org/10.1046/j.1440-1819.2002.00999.x

Wehrle, R., Kaufmann, C., Wetter, T. C., Holsboer, F., Auer, D. P., Pollmächer, T., & Czisch, M. (2007). Functional microstates within human REM sleep: first evidence from fMRI of a thalamocortical network specific for phasic REM periods. *European Journal of Neuroscience*, *25*(3), 863-871.

Wielek, T., Blume, C., Wislowska, M., del Giudice, R., & Schabus, M. (2021). Decoding Brain Responses to Names and Voices across Different Vigilance States. *Sensors*, *21*(10), 3393. https://www.mdpi.com/1424-8220/21/10/3393